PARTITIONLESS CRYSTALLIZATION AND GLASS FORMATION IN Fe-B ALLOYS DURING PICOSECOND PULSED LASER QUENCHING

F. Spaepen and C.J. Lin

Division of Applied Sciences, Harvard University, Cambridge, MA 02138, U.S.A.

Reprinted from

Amorphous Metals and Non-Equilibrium Processing
MRS Symposia Proceedings, M. von Allmen, editor,
Les Editions de Physique (Les Ulis, France), 1984.

PARTITIONLESS CRYSTALLIZATION AND GLASS FORMATION IN Fe-B ALLOYS DURING PICOSECOND PULSED LASER QUENCHING

F. Spaepen and Chien-Jung Lin*

Division of Applied Sciences, Harvard University, Cambridge, MA 02138, U.S.A.

Résumé - La vitrification, par trempe laser à impulsions picosecondes, des alliages Fe-B contenant au moins 5 at.% de B est expliquée quantitativement par la transition d'une croissance cristalline limitée par collision atomique, à une croissance limitée par diffusion atomique. La ligne T_o pour la solidification de la phase c.c. dans le liquide, sans redistribution des constituants, est calculée en utilisant la théorie des solutions régulières et le diagramme des phases.

Abstract - Glass formation in picosecond laser quenching of Fe-B alloys containing a minimum of 5 at.% B is explained quantitatively by a transition from collision-limited to diffusion-limited crystal growth. The T_o line for partitionless growth of the fcc phase from the liquid is calculated from regular solution theory and the equilibrium phase diagram.

1 - INTRODUCTION

The process of energy deposition, heating and cooling in pulsed laser processing has been discussed in detail by Bloembergen [1] and others [2-4]. Figure 1 illustrates

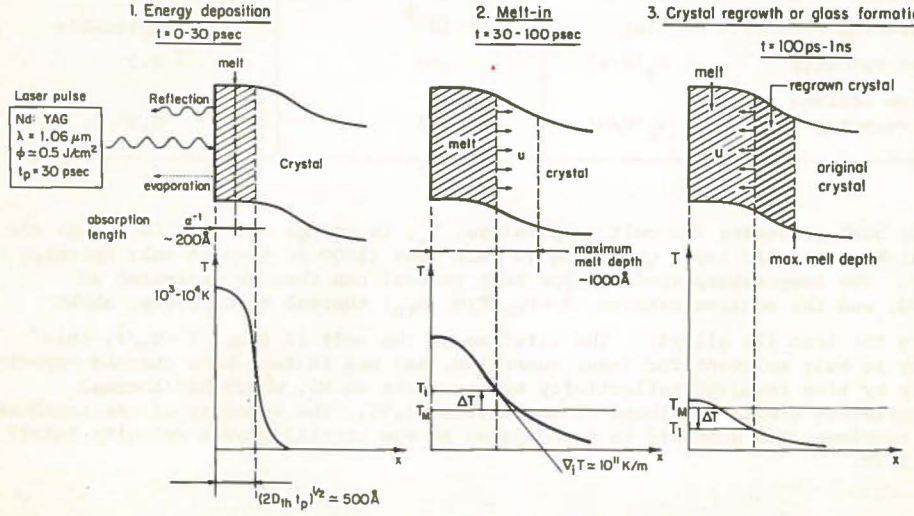

Fig. 1 - *Schematic diagrams illustrating the mechanism of pulsed laser quenching.*

the main stages of this process in a typical picosecond pulsed laser experiment: (i) energy deposition in a layer on the order of the absorption depth (200 Å), which spreads by heat conduction over a layer of thickness $(2D_{th}t_p)^{1/2}$ of about 500 Å

*Present address: IBM Research Laboratory, 5600 Cottle Road, San Jose, CA 95193.

(D_{th}: thermal diffusivity; t_p: laser pulse length); since energy losses due to evaporation are negligible [4], this layer melts and its temperature rises to several thousand degrees; (ii) during the melt-in period, this overheat is spent as heat of fusion of more substrate crystal to a total thickness of about 1000 Å; due to the very high thermal gradients, the estimated melt-in velocity is extremely large (~1000 m/s); (iii) when the maximum melt depth is reached, the crystal melt interface reverses direction; depending on the relative rates of crystal growth and heat removal, the molten layer solidifies as a regrown crystal or a glass. The competition between the latter processes are analyzed in detail in this paper for the Fe-B system.

2 - THERMAL PARAMETERS

Although a number of sophisticated analyses of the heat flow during laser quenching are available, the order of magnitude of most of the relevant quantities can easily be estimated from essentially dimensional arguments. They are listed in Table I, together with the corresponding values for melt spinning. The starting point is

Table I

THERMAL PARAMETERS IN MELT QUENCHING

		Laser Quenching	Melt Spinning
Melt temperature	T_m(K)	10^3	10^3
Melt thickness	d(m)	10^{-7}	5×10^{-5}
Temperature gradient	∇T(K/m)	10^{10}	2×10^7
Cooling rate	$\dot{T}$(K/s)	10^{12}	4×10^6
Melt lifetime	τ(s)	10^{-9}	not applicable
Isotherm velocity	u_T(m/s)	100	0.2
Heat-flow limited crystal growth velocity	u_h(m/s)	230	0.5

that for both processes the melt temperature, T_m, is on the order of 10^3K, but the melt thickness, d, in laser quenching is much less (1000 Å) than in melt spinning (50 μm). The temperature gradient for heat removal can then be estimated as $\nabla T = T_m/d$, and the cooling rate as $\dot{T} = D_{th}\nabla T/d$ (D_{th}: thermal diffusivity, about 10^{-5} m^2/s for iron its alloys). The lifetime of the melt is then $\tau = T_m/\dot{T}$; this quantity is only relevant for laser quenching, and has in fact been checked experimentally by time resolved reflectivity measurements on Si, which has thermal characteristics similar to those of the metals [5,6]. The velocity of the isotherms in the specimen (the quantity to be compared to the crystal growth velocity later) is $u_T = \dot{T}/\nabla T$.

3 - THERMODYNAMICS AND KINETICS OF CRYSTAL GROWTH

The crystal growth velocity is determined by the balance of the removal of the heat of crystallization, ΔH, and the kinetics of the atomic processes at the interface. The heat flow limited crystal growth velocity is:

$$u_h = \frac{K\bar{V}\nabla T}{\Delta H} \qquad (1)$$

(κ: thermal conductivity; $\bar{V}$ molar volume). Table I lists typical values for Fe, using $\Delta H = 15$ kJ/mole, $\kappa = 50$ W/m·K, and $\bar{V} = 7.1 \times 10^{-6}$ m^3/mole.

The crystal growth velocity depends on the interface kinetics and the thermodynamic driving force as follows [2]:

$$u = u_o\left[1 - \exp\left(\frac{\Delta G}{RT}\right)\right] \tag{2}$$

where ΔG is the free energy difference between crystal and melt, and the prefactor, u_o, depends on the nature of the atomic rearrangement needed for incorporation of a liquid atom into the crystal. If only simple collision of liquid atoms with the crystal surface is required (as in pure metals), the atomic jump frequency is the vibrational frequency in the liquid, so that u_o in this case is close to the speed of sound, u_s, in the liquid. In the analysis below, a rough, estimated value of 3500 m/s, independent of temperature, is used for u_s. If incorporation of the atoms in the crystal requires diffusional jumps (i.e., changes of nearest neighbors), u_o is approximately equal to D/λ (D: diffusivity in the liquid; λ: jump distance, taken as 2.6×10^{-10} m in Fe-based alloys). Note that diffusion-limited crystal growth does not necessarily imply long-range atomic transport; changes in short-range order that require changes in coordination can also only occur by diffusional jumps. The diffusivity used in the analysis below has the Fulcher-Vogel form, typical of liquid metal alloys:

$$D = D_o \exp\left(-\frac{B}{T - T'_o}\right) \tag{3}$$

with $D_o = 1.4 \times 10^{-8}$ m^2/s, $T'_o = 581$K, and $B = 1300$K.

The value of B is a rough estimate, similar to that observed in measurements on other metallic glasses and consistent with the free volume model [7]. D_o and T'_o were then calculated by assuming $D = 5 \times 10^{-9}$ m^2/s at the melting point of iron (1807K), and $D = 10^{-16}$ m^2/s at the crystallization temperature of B-rich Fe-B glasses (650K) [8].

Since the isotherm speed is several 100 m/s in the ps laser quench, the crystal growth velocity, u, must be at least this high to prevent glass formation. The time required to crystallize a monolayer at this speed, λ/u, is less than 1 ps. The distance an atom can diffuse in that amount of time, $(D\lambda/u)^{1/2}$, is then less than an interatomic distance. Crystallization must therefore be *partitionless*, i.e., without change in composition. In alloys, partitionless crystallization at a particular composition is thermodynamically possible only below a temperature, T_o, at which the free energies of melt and crystal are equal.

Assuming a simple regular solution model for both melt and crystal, the driving free energy for partitionless crystallization of an Fe-B alloy melt to a supersaturated b.c.c. phase is

$$\Delta G = G_c - G_\ell = x_{Fe}\Delta\mu^o_{Fe} + x_B\Delta\mu^o_B + x_{Fe}x_B(\varepsilon_c - \varepsilon_\ell) \tag{4}$$

(G_c, G_ℓ: free energies of crystal and liquid, respectively; x_{Fe}, x_B: atom fractions of Fe and B; ε_c, ε_ℓ: regular solution interaction parameters).

The standard free energy difference can be approximated by:

$$\Delta\mu^o_i = \mu^o_{i,c} - \mu^o_{i,\ell} = \Delta S_{f,i}(T - T_{M,i}) \tag{5}$$

($\Delta S_{f,j}$: entropy of fusion, and $T_{M,i}$: melting temperature of element i). The T_o temperature is found by setting ΔG equal to zero, which gives:

$$T_o = \frac{x_{Fe}x_B(\varepsilon_c-\varepsilon_\ell)+x_{Fe}T_{M,Fe}\Delta S_{f,Fe}+x_BT_{M,B}\Delta S_{f,B}}{x_{Fe}\Delta S_{f,Fe}+x_B\Delta S_{f,B}} \quad (6)$$

The interaction parameters can be determined by equating the chemical potentials of Fe and B at the equilibrium liquid and crystal compositions, which can be found on the phase diagram. For the Fe-B systems, $\varepsilon_c - \varepsilon_\ell$ was calculated to be -92 kJ/mole, independent of temperature. The other parameters can be found in all standard references [9]: $\Delta S_{f,Fe} = 7.6$ J/K mole; $\Delta S_{f,B} = 21.8$ J/K mole; $T_{M,Fe} = 1807$K; $T_{M,B} = 2300$K. The result is shown in Fig. 2. Note that only the b.c.c. phase is

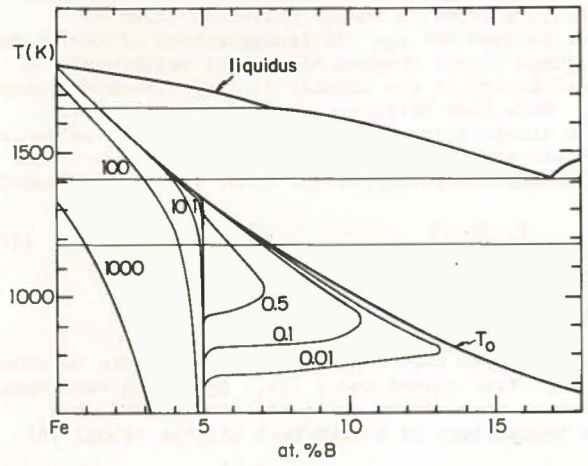

Fig. 2 - *The Fe-B phase diagram. The T_o line corresponds to the liquid→b.c.c. transition. The contours represent the crystal growth speed (in m/s) as a function of composition and interface temperature.*

being considered here; the f.c.c. Fe phase does not nucleate or grow. Inserting Eq. (6) into Eq. (4) gives an expression for the driving force.

$$\Delta G = (x_{Fe}\Delta S_{f,Fe} + x_B\Delta S_{f,B})(T - T_o) \quad (7)$$

Some authors [10,11] have assumed that partitionless crystallization is always a very fast process, and that therefore glass formation below the T_o line is prohibited. The Fe-B system is one of many in which this has experimentally been disproved.

4 - EXPERIMENTAL RESULTS

Fe-B glasses have been prepared by melt spinning in the 12-28 at.%B range [8,12,13]. Below 12 at.%B a b.c.c. supersaturated solution is formed. It is interesting to note that upon heating glasses with less than 18 at.%B first crystallize to the metastable b.c.c. solution, which then converts to the stable phase mixture of α-Fe and Fe_3B [8]. Our calculation shows that the composition corresponding to $T_o = 660$K (the crystallization temperature for an 18 at.%B glass) is 16 at.%B. Considering the approximate nature of the regular solution models, this agreement is quite satisfactory.

Glass formation in the Fe-B system has been studied under ps laser quenching conditions, using the following experimental technique [14,15]. On a copper substrate, first coated with a 1 μm thick Al film, a 1000 Å thick compositionally modulated film consisting of alternate layers of Fe and $Fe_{76}B_{24}$ was deposited by dual target

DC sputtering. The repeat length of the modulation was about 20 Å. By varying the relative thicknesses of the Fe and $Fe_{76}B_{24}$ layer, films with average compositions between 0 and 24 at.%B were prepared. These samples were irradiated with a 30 ps Nd:YAG ($\lambda = 1.06$ μm) laser pulse, with a beam diameter of about 100 μm and an average fluence of about 0.8 J/cm^2. The composition modulation wavelength was chosen on the order of the mixing length $(D\tau)^{1/2}$ in the liquid during the lifetime of the melt ($\tau = 1$ ns, Table I), to ensure homogeneity. After dissolution of the Al film in dilute NaOH, the irradiated film could be investigated directly by transmission electron microscopy without further thinning.

These experiments showed that ps laser quenching results in glass formation in alloys containing at least 5 at.%B. Alloys containing less than 5 at.%B crystallized as a b.c.c. solid solution. The solidification morphology of the 4 at.%B contained a small amount of glass/crystalline mixture near the top surface of the film [16]; this could have been the result of an interfacial instability that became possible at the last stages of solidification due to the decrease in the crystal growth velocity [17]; the associated redistribution of B then could result in glass formation in the B-rich regions.

5 - ANALYSIS

The sharp transition from partitionless crystal growth to glass formation at 5 at.%B can most easily be explained by a transition from a collision-controlled to a diffusion-controlled crystal growth mechanism. The short-range order in a metal-metalloid glass such as Fe-B, and hence also in the very undercooled melt, is known to be quite strong: each metalloid is surrounded by metal atoms only, in a coordination shell similar to that found in the intermetallic compounds [18,19]. The short-range order around the B atom in the b.c.c. solution, either substitutional or interstitial, is clearly very different. Reconstruction of the cluster containing the B atom therefore requires diffusive jumps. The formation of a glass with a minimum of 5 at.%B suggests that the size of this cluster is 20 atoms (i.e., each B atom and 19 of its nearest neighbors, which corresponds to the first and about half the second coordination shell of the B-atom [20]). The Fe atoms outside these clusters are assumed to make collisional jumps. The kinetic factor in Eq. (2) for the crystal growth speed can therefore be written for $x_B \leqslant 0.05$:

$$u_o = (20\ x_B)\ \frac{D}{\lambda} + (1-20\ x_B)u_s \quad . \tag{8}$$

For $x_B \geqslant 0.05$, the crystal growth speed is equal to the diffusive speed D/λ.

Figure 2 shows contours of the crystal growth speed, u, as a function of interface temperature and composition. The abrupt transition at 5 at.%B is obvious. Figure 3 shows as a function of composition, the total distance grown by the crystal if cooled at a constant rate form the liquidus temperature to 600K. The scale on the left hand side is for the "master curve" representing the product of this distance and the cooling rate. On the right hand side, the actual growth distances in melt spinning and laser quenching are shown. At 5 at.%B, the growth distance in ps laser quenching is on the order of 10 Å; most of a 1000 Å thick layer is therefore transformed to a glass, as observed in our experiments. At 12 at.%B, the growth distance in melt spinning is on the order of 1 μm, consistent with the experimentally observed glass formation in 50 μm thick ribbons. Figure 4 illustrates the same points in a slightly different way. For pure Fe and the 4 at.%B alloy, the crystal growth velocity rises above the isotherm velocity in ps laser quenching, thus preventing glass formation. For 5 at.%B, the crystal growth velocity rises above the isotherm velocity in melt spinning, but remains below the one in laser quenching. This is consistent with glass formation at this composition under the latter conditions, and failure to form a glass under the former. The crystal growth velocity for the 12 at.%B alloy lies below the isotherm velocity for melt spinning, in agreement with the observations.

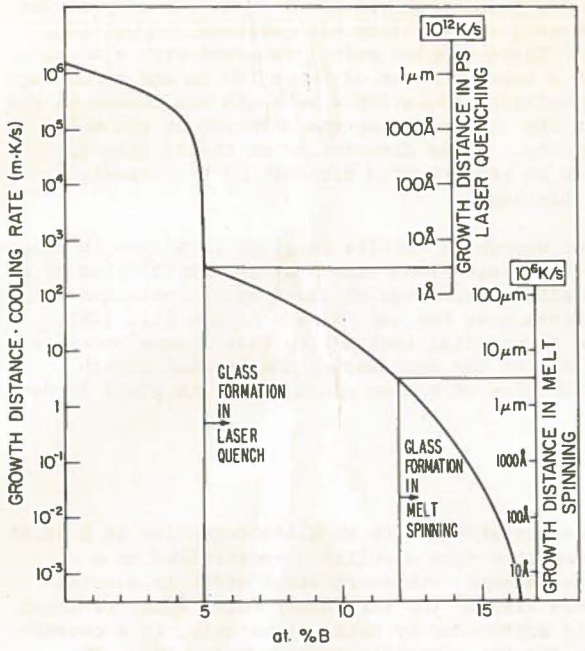

Fig. 3 - *Crystal growth distance upon continuous cooling of an* Fe-B *alloy, as a function of composition (see text for explanation of scales).*

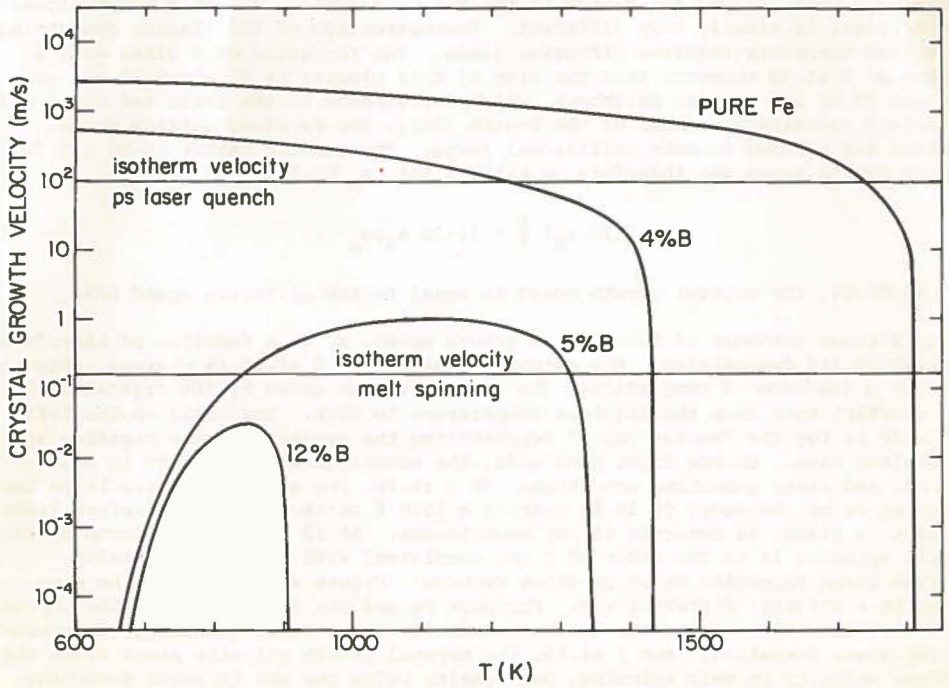

Fig. 4 - *Crystal growth velocity as a function of interface temperature for four compositions in the* Fe-B *system.*

There exists experimental support for the very large growth velocities for pure Fe shown on Fig. 4. In ps laser annealing experiments on pure Fe, the original sputtered film had a grain size of 500 Å. After irradiation the grain size was 1 μm or more [15,21]. Since these grains had to grow within the 1 ns lifetime of the melt, the lateral growth velocity must have been at least 500 m/s; the velocity may in fact be considerably larger yet, since the lateral growth is limited to the very early stages of the crystallization. Coriell and Turnbull [22] also found a very large kinetic factor, on the order of the speed of sound, in their analysis of dendritic growth velocity measurements in very undercooled Ni melts.

6 - CONCLUSIONS

The ps laser quenching experiments on Fe-B alloys have demonstrated that metallic glasses can be formed far below the T_o-line. This has also been observed in the Ni-Nb, Mo-Ni and Mo-Co systems [3]. Partitionless crystallization is therefore not necessarily a fast mechanism that forestalls glass formation as some authors have claimed [10,11]. For the Fe-B system, the glass formation range can be qualitatively accounted for by a transition from collision-controlled to diffusion-controlled crystallization at 5 at.%B. The analysis gives sensible values for the glass formation range in melt spinning as well. Detailed quantitative agreement on the latter process cannot be claimed, however, since the results at low temperature depend rather sensitively on the choice of the parameters in the Fulcher-Vogel equation for the diffusion coefficient. Crystal nucleation, which is probably more important in melt spinning than in laser quenching, has not been considered here. Unless the conditions are right for copious homogeneous nucleation (including the transient effects [23]), taking into account nucleation effects will result in a decrease of the fraction crystallized.

ACKNOWLEDGMENTS

This work has been supported by the Office of Naval Research under Contract No. N00014-83-K-0030.

REFERENCES

1. N. Bloembergen, in "Laser-Solid Interactions and Laser Processing," eds. S.D. Ferris, H.J. Leamy, and J.M. Poate, AIP, N.Y. (1979), p. 1.

2. F. Spaepen and D. Turnbull, in "Laser Processing of Semiconductors," eds. J.M. Poate and J.W. Mayer, Academic, N.Y. (1982), p. 15.

3. C.J. Lin, F. Spaepen, and D. Turnbull, J. Non-Cryst. Solids, 61/62, 767 (1984).

4. C.J. Lin and F. Spaepen, in "Rapidly Solidified Metastable Materials," eds. B.H. Kear and B.C. Giessen, MRS Symp. Proc., North-Holland, Amsterdam (1984), in press.

5. J.M. Liu, Ph.D. Thesis, Harvard University (1982).

6. A.L. Lompré, J.M. Liu, H. Kurz, and N. Bloembergen, in "Energy Beam-Solid Interactions and Transient Thermal Processing," eds. J.C.C. Fan and N.M. Johnson, MRS Symp. Proc., North-Holland, Amsterdam (1984), in press.

7. F. Spaepen and A.I. Taub, in "Amorphous Metallic Alloys," ed. F.E. Luborsky, Butterworths, London (1983), p. 231.

8. R. Hasegawa and R. Ray, J. Appl. Phys., 49, 4174 (1978).

9. R. Hultgren, P.D. Desai, D.T. Hawkins, M. Gleiser, K.K. Kelley, and D.D. Wagman, "Selected Values of the Thermodynamic Properties of the Elements," ASM, Cleveland (1973).

10. T.B. Massalski, Proc. 4th Int. Conf. on Rapidly Quenched Metals, eds. T. Masumoto and T. Suzuki, Jap. Inst. Metals, Sendai (1982), p. 203.

11. W.J. Boettinger, *ibid.*, p. 99.

12. R. Ray and R. Hasegawa, Sol. St. Comm., 27, 471 (1978).

13. F.E. Luborsky and H.H. Liebermann, Appl. Phys. Lett., 33, 233 (1978).

14. C.J. Lin and F. Spaepen, Appl. Phys. Lett., 41, 721 (1981).

15. C.J. Lin and F. Spaepen, in "Chemistry and Physics of Rapidly Solidified Materials," eds. B.J. Berkowitz and R. Scattergood, TMS-AIME, N.Y. (1983), p. 273.

16. C.J. Lin and F. Spaepen, Scripta Met., 17, 1259 (1983).

17. J.W. Cahn, S.R. Coriell, and W.J. Boettinger, in "Laser and Electron Beam Processing of Materials," eds. C.W. White and P.S. Peercy, Academic, N.Y. (1980), p. 89.

18. G.S. Cargill III, Solid State Physics, 30, 227 (1975).

19. P.H. Gaskell, in "Glassy Metals II," eds. H. Beck and H.J. Güntherodt, Springer, Berlin (1983), p. 5.

20. E. Nold, P. Lamparter, H. Olbrich, G. RAiner-Harbach, and S. Steeb, Z. Naturforsch., 36A, 1032 (1981).

21. C.J. Lin, Ph.D. Thesis, Harvard University (1983).

22. S.R. Coriell and D. Turnbull, Acta Met., 30, 2135 (1982).

23. K.F. Kelton, A.L. Greer, and C.V. Thompson, J. Chem. Phys. 79, 6261 (1983).